Effects of nonstoichiometry, ordering, and Bi substitution with Pb in $Bi_2Sr_2CaCu_2O_8$

L. Szunyogh,* G. Hörmandinger, and P. Weinberger
Institut für Technische Elektrochemie, Technische Universität Wien, Getreidemarkt 9/158, A-1060 Vienna, Austria
(Received 24 September 1990)

The fully relativistic real-space scattering cluster coherent-potential approximation is applied to $Bi_2Sr_2CaCu_2O_{8-\delta}$ for $0 \le \delta \le 0.5$ with respect to each oxygen sublattice and to $(Bi_{1-x}Pb_x)_2Sr_2CaCu_2O_8$ for $0 \le x \le 0.25$. Increasing ε_F was found as the vacancy content increases, while $n(\varepsilon_F)$ is decreased by disorder in the O(1) sublattice (Cu-O layers) and increased due to vacancies in the O(2) sublattice (Bi-O layers). As in the Y-Ba-Cu-O system, the effective oxygen-oxygen pair interactions in the Cu-O plane indicate the creation of "isolated" Cu ions. By "doping" the Bi sublattice with Pb, ε_F drops and $n(\varepsilon_F)$ increases. From the effective Bi-Bi pair interactions an (antilikewise) ordering of Bi and Pb atoms can be deduced. Calculated x-ray-emission and uv-photoemission intensities for the nonstoichiometric system are presented.

I. INTRODUCTION

The superconducting Bi-Sr-Ca-Cu-O system has been studied extensively during the last two years. Several $Bi_2Sr_2Ca_{n-1}Cu_nO_y$ politypoids have been identified with different superconducting transition temperatures,[1-4] but only for the $n=1$ (2:2:0:1) and $n=2$ (2:2:1:2) phases could single crystals be obtained with $T_c=7$–22 and 75–85 K, respectively, while the $n=3$ phase (2:2:2:3) with $T_c=110$ K is stable only by partially replacing Bi by Pb.[5-7] The substitution of Pb on the Bi sites, therefore, seems to be a dominating effect in modifying the thermodynamics of these systems.[8] As far as the crystal structure is concerned, a face-centered orthorhombic subcell ($b=1.000\,78a$, $c=8a$) was determined with an approximate $2\times5\sqrt{2}$ superlattice formation in the a–b plane.[4,5] In the 2:2:1:2 phase, both the addition and the removal of oxygen decrease T_c with respect to the stoichiometric composition.[9,10] When decreasing the oxygen content, a metal-insulator transition is observed as confirmed by also decreasing Hall numbers (effective charge carriers).[10,11] Nevertheless, a set of data of physical quantities as a function of precise oxygen content has not yet been presented.

Subsequently, a considerable number of local-density-approximation (LDA) band-structure calculations for $Bi_2Sr_2CaCu_2O_8$ have been published using the linearized muffin-tin orbital method in the atomic-sphere approximation (LMTO-ASA),[12,13] the pseudofunction method,[14] or the full-potential linearized augmented-plane-wave method (FLAPW).[15-17] Note that, in all of these calculations, a body-centered tetragonal[12-16] or a face-centered orthorhombic[17] crystal structure was assumed to be neglected thus, the superlattice effects. In agreement with the notation used in Ref. 17, we shall refer to the oxygen positions in the Cu-O, Bi-O, and Sr-O layers as O(1), O(2), and O(3), respectively. Owing to the small dispersion along the c axis, the resulting band structure shows a highly two-dimensional character. The striking features of the valence band can be summarized as follows: (a) widely dispersed ($\sim$9 eV) bands mainly below the Fermi energy related to the Cu d and O(1) $p\,\sigma$ bonds, (b) Cu-O(1)-O(3) $dp\pi$ bands resulting in two major peaks in the density of states (DOS) around -1.4 and -3.6 eV, (c) Bi p and O(2) $p\,\sigma$ bonds with strong ionic character, thus indicating an asymmetric weight of mainly O(2) p-like states below ε_F and Bi p-like states from -0.3 eV below to 3.6 eV above ε_F, and (d) strongly interacting (antibonding) Bi-O(2)-O(3) and Cu-O(1) bands at the Fermi surface giving rise to highly hybridized and localized states at ε_F.

Although the experimental valence-band photoelectron spectra suggest a metallic-like character for the normal state of the 2:2:1:2 phase,[18-21] probably due to large correlation effects in the Cu-O layers, the calculated angle-integrated LDA photoelectron spectra[22] deviate considerably from the experimental data. In the vicinity of the Fermi surface, the bandstructure deduced from angle-resolved photoemission spectra is in reasonable agreement with the theoretical one; the experimental binding energies, however, are by about 0.3 eV lower than those calculated in terms of the density-functional theory.[23-25] An attempt to improve the agreement between experiment and theory has been made very recently by Hörmandinger *et al.*[26] performing a fully relativistic Korringa-Kohn-Rostocker (RKKR) calculation on $Bi_2Sr_2CaCu_2O_8$. As expected, the bands below the Fermi level having less Bi character remain practically unchanged compared to the scalar-relativistic bands. The bands above ε_F having dominantly Bi p character, however, are split by about 1 eV pushing an increased weight of these states into the occupied region which, in turn, results in a dropping of ε_F by about 0.14 eV. Consequently, near the Fermi level this improves the agreement with the experimentally observed band structure.

Burgäzy *et al.*[27] have presented O K_α x-ray-emission spectroscopy (XES) experiments for $Bi_2Sr_2CaCu_2O_8$. They have found satisfactory agreement with the calcu-

 ©1991 The American Physical Society

lated LDA spectrum[22] when putting the O(2) and O(3) 1*s* binding energies, as computed by Massidda *et al.*,[17] at an equal level and by shifting the O(1) 1*s* binding energy by about 0.5 eV below this level. This deviation has been attributed to the more ionic nature of the Bi—O bond than inferred from the band-structure calculations or to the smaller length of this bond than assumed.

II. THEORY AND COMPUTATIONAL DETAILS

The concept of the real-space scattering cluster coherent-potential approximation (RSSC-CPA) has been discussed previously.[28] In the fully relativistic case, the corresponding equations for the scattering path operator are formally identical to the nonrelativistic case [see Eqs. (1) and (2) of Ref. 28], the occurring angular-momentum representations, however, are labeled by the relativistic quantum numbers κ and μ:

$$\underline{t}_i(\varepsilon)=\{t_{i,QQ'}(\varepsilon)\},\quad \underline{G}^{ij}(\varepsilon)=\{G^{ij}_{QQ'}(\varepsilon)\}\ , \tag{1}$$

$$Q=(\kappa,\mu),\quad \kappa=\begin{cases}-l-1, & j=l+\frac{1}{2}\\ l, & j=l-\frac{1}{2}\end{cases},\quad -j\le\mu\le j\ .$$

In (1), $\underline{t}_i(\varepsilon)$ are the (relativistic) single-site t matrices and $\underline{G}^{ij}(\varepsilon)$ are the (relativistic) structure constants,

$$G^{ij}_{QQ'}(\varepsilon)=\sum_{s=\pm1/2} c(lj1/2;\mu-s,s) \times G^{nr,ij}_{LL'}(\varepsilon)c(l'j'1/2;\mu'-s,s)\ , \tag{2}$$

where $G^{nr,ij}_{LL'}(\varepsilon)$ refers to the nonrelativistic structure constants, $c(lj1/2;\mu-s,s)$ denotes Clebsch-Gordan coefficients, ε is the energy, and i,j denote sites. For a detailed description see Secs. 5.3.2 and 6.1.2 of Ref. 29. Similar to the nonrelativistic formalism, from the κ-like partial local densities of states (LDOS) and κ-like partial cross sections, one can compute spectroscopic intensities [XES, photoemission spectroscopy PES)] (see, e.g., Secs. 11.3.2 and 11.4.2 of Ref. 29). Furthermore, the calculation of effective (cluster) pair interactions[30] is also straightforward within a relativistic formalism.

In the present calculations we used the muffin-tinized self-consistent potentials of Massidda *et al.*[17] The vacancy and the lead potentials were approximated by matching the potentials derived from the concentration weighted superposed ionic charge densities to the self-consistent potentials as described in Ref. 31, whereby formal ionicities of Bi^{3+}, Sr^{2+}, Ca^{2+}, Cu^{2+}, and O^{2-} were assumed. Because of the non-self-consistent way of this potential construction, the long-range Madelung-type effects (charge waves) could be estimated merely due to the concentration-dependent superposition of the charge densities. It should be noted that the vacancy site, represented by a rather flat positive potential, is basically an *s* scatterer, which, in turn, is not described by a resonant-like phase shift, i.e., a phase-shift crossing sharply through $\pi/2$ as a function of energy. As studied in Ref. 32, the calculated physical quantities are fairly insensitive with respect to the shape of such vacancy potentials. Similarly, the *p*-like phase shift corresponding to the lead potential shows no resonance, its flat maximum is indeed well beyond the occupied region of the valence band. Concomitantly, we do not expect essential changes of the calculated physical properties (spectroscopical intensities, effective pair interactions) due to a more sophisticated (self-consistent) way of potential construction.

A cluster of exactly 100 sites in a sphere with a radius of 15 Å centered around the bisecting point of a Bi—Bi bond between two neighboring Bi-O layers was found to be sufficient for reliable LDOS's and effective scattering amplitudes. The radii used for the radial integration[28] are $R_{Bi}=R_{Sr}=R_{Ca}=2.85$ a.u., $R_{Cu}=2.0$ a.u., and $R_{O(1)}=R_{O(2)}=R_{O(3)}=3.08$ a.u. The method of Ginatempo and Staunton[33] has been employed for solving the CPA condition for the effective scattering amplitudes (10^{-5} deviation for each matrix element between two successive steps). The calculations were performed along the real energy axis for the nonstoichiometric system and with an imaginary part for the energy of 2 mRy in the case of the Pb substitution. In the latter case, the scattering path operator and the effective scattering amplitudes have been deconvoluted to the real axis by means of the Rieman-Cauchy condition. An inequidistant energy mesh of nearly 200 points was used from -5.4 eV (zero level of the muffin-tin potentials) up to 4 eV with respect to the FLAPW Fermi level.[17]

In what follows we denote by "*nonstoichiometric*" the case when the "law of constant proportions" is not resolved in terms of integer numbers as for $Bi_2Sr_2CaCu_2O_{8-\delta}$ ($0<\delta\le0.5$). Since, in this case, the components of a particular sublattice, namely, vacancies and oxygen atoms, are assumed in the CPA to be distributed randomly, as in a binary substitutional alloy, we speak about a *disordered* oxygen sublattice, in the same way as about a disordered bismuth sublattice in the case of $(Bi_{1-x}Pb_x)_2Sr_2CaCu_2O_8$.

III. RESULTS

A. $Bi_2Sr_2CaCu_2O_8$

As a first step we carried out a scalar-relativistic calculation for the ordered system. Our scalar-relativistic DOS's show an overall good agreement with the muffin-tin-projected DOS's of the (semirelativistic) FLAPW calculation.[17] The integrated total muffin-tin DOS at the FLAPW Fermi level for our scalar-relativistic calculation compares, within an error of 0.6%, to that obtained from the FLAPW method, while the total number of electrons computed using the enlarged oxygen spheres[28] yields only 65.2 electrons at ε_F^{FLAPW}, which is by 0.8 electron less than required. While the FLAPW Fermi energy is thought to be correct for our scalar-relativistic calculation, this missing charge Δ is considered as a constant correction to all integrated cluster DOS (Ref. 28) and is attributed to the incomplete description of the interstitial region within a cluster model.

The relativistic DOS's for the ordered system differ from their scalar-relativistic counterparts due to the spin-orbit splitting only in the Bi *p*-like LDOS and, consequently, because of the strong hybridization, also in the O(2) and O(3) *p*-like LDOS's. This is clearly illustrated in

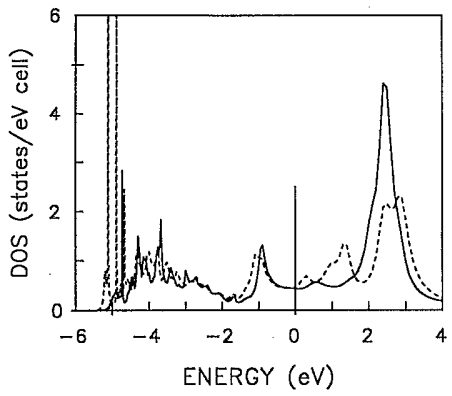

FIG. 1. Scalar-relativistic (solid line) and relativistic (dashed line) LDOS of Bi for the stoichiometric case.

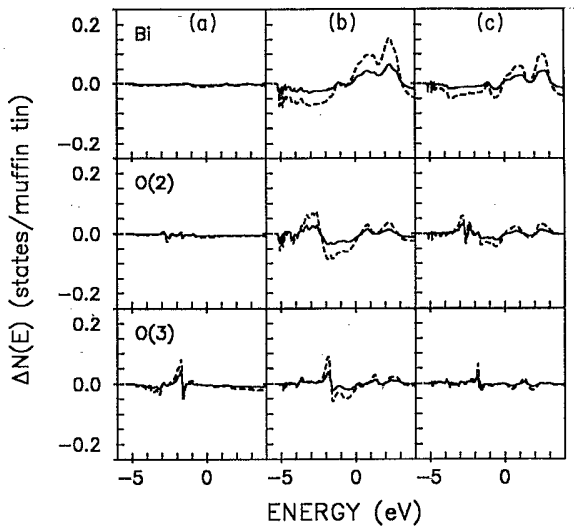

FIG. 2. Differences of the integrated LDOS's in $Bi_2Sr_2CaCu_2O_{8-\delta}$ relative to the ordered system as a function of the energy for Bi (upper sheet), O(2) (middle sheet), and O(3) (lower sheet). The labels (a), (b), and (c) refer to a disordered O(1), O(2), and O(3) sublattice, respectively. The solid line corresponds to $\delta=0.2$, the dashed line to $\delta=0.5$.

Fig. 1 showing a spin-orbit splitting of about 1.3 eV in the Bi LDOS above ε_F. Since the weight of gravity of these states is shifted downwards by about 0.5 eV, a small downward shift is also seen for the states just below ε_F. This implies a dropping of the calculated Fermi energy by 0.12 eV with respect to the scalar-relativistic case. This is in full agreement with the result of Hörmandinger *et al.*[26] In addition, $n(\varepsilon_F)$ increases from 3.14 states/(eV cell) for the scalar-relativistic case to 3.75 states/(eV cell) for the relativistic case.

The states at about -5 eV are also shifted downwards (see also, Fig. 3 of Ref. 26), thus coming very close to the zero level of the muffin-tin potentials. Considering no bound states in the real-space (finite cluster) Green's-function theory, the diagonal elements of the scattering path operator are real for negative energies (see also, Beeby,[34]), and therefore the entire valence band has to lie in the positive-energy region, i.e., above -5.4 eV with respect to ε_F in the present case. Since the number of electrons in the valence band is given independently from the method of calculation by Lloyd's integrated DOS, in the vicinity of the zero level of the muffin-tin potentials very sharp peaks can occur in the DOS to account for the correct behavior of the integrated DOS. This explains the artificially sharp peeks at -5 eV in the relativistic LDOS of Bi seen in Fig. 1.

B. $Bi_2Sr_2CaCu_2O_{8-\delta}$

We have performed relativistic CPA calculations for all three different oxygen sublattices in the concentration range of $0\leq\delta\leq0.5$. The main changes in the electronic structure can be monitored in the difference, ΔN, between the muffin-tin-projected integrated LDOS for the disordered case and the ordered case, which is plotted as a function of the energy for the Bi, O(2), and O(3) as well as for the Cu and O(1) sites in Figs. 2 and 3, respectively. Apparently, vacancies on the O(1) sublattice induce negligible effects on the Bi-O layers and, concomitantly, disorder on the O(2) sublattice leaves nearly uneffected the states related to the Cu-O planes. However, the states attributed to the O(3) site interact with those of both the Bi-O and the Cu-O layers. The overall features are closely related to the nonstoichiometric Y-Ba-Cu-O system in so far as the Cu-O, Sr-O, and Bi-O layers in $Bi_2Sr_2CaCu_2O_8$ correspond to the Cu-O, Ba-O layers, and Cu-O chains in $YBa_2Cu_3O_7$, respectively. The crucial difference between these two compounds is that, while the Cu(1) states (chain) in the Y-Ba-Cu-O system are occupied, the Bi states lie mainly in the unoccupied energy region. Therefore, disorder in the Bi-O layers (and also

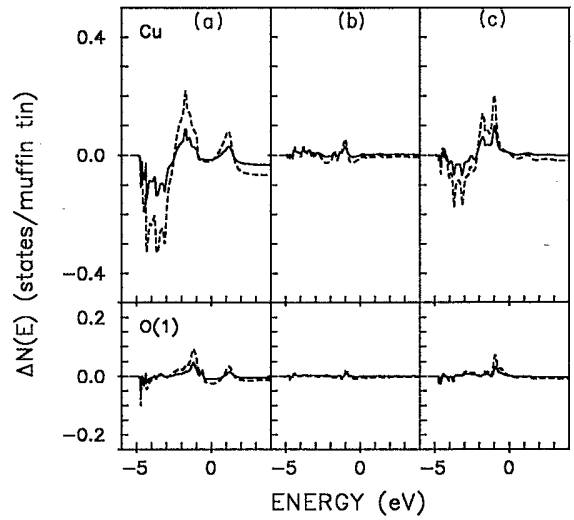

FIG. 3. Differences of the integrated LDOS's in $Bi_2Sr_2CaCu_2O_{8-\delta}$ relative to the ordered system as a function of the energy for Cu (upper sheet) and O(1) (lower sheet). The labels (a), (b), and (c) refer to a disordered O(1), O(2), and O(3) sublattice, respectively. The solid line corresponds to $\delta=0.2$, the dashed line to $\delta=0.5$.

in the Sr-O layers) effect the Bi states mainly above ε_F. The two major peaks above ε_F in the Bi LDOS [and also in the O(2) and O(3) LDOS's] are broadened due to disorder. This leads to an increased weight of states related to Bi, O(2), and O(3) at ε_F if the O(2) sublattice is partially occupied by vacancies. For a disordered O(3) sublattice, this broadening is less pronounced. Since the Cu—O bonds are partially broken, in the case of the O(1) and O(3) vacancies, the weight of the nonbonding Cu d states at energies -3—-2 eV is increased.

The calculated Fermi energies and DOS's at the Fermi energy for the nonstoichiometric Bi-Sr-Ca-Cu-O system are shown in Table I as the difference with respect to the stoichiometric case. The steady increase of ε_F seems to partially follow a rigid-band behavior: the increase of ε_F reflects the charge difference between a negative oxygen ion and a neutral oxygen atom. The modifications of the electronic states discussed in the previous paragraph merely have a secondary effect on ε_F. Due to the hybridization with Bi p-like states, for O(2) and O(3), a larger amount of states is unoccupied than for O(1). Consequently, the removal of oxygen atoms from the O(1) sublattice increases ε_F the most. The decreasing contribution of the O(1) partial density of states (PDOS) also explains the dropping of $n(\varepsilon_F)$ for a disordered O(1) sublattice. Nevertheless, for the disordered O(2) and O(3) sublattices the rigid-band model alone cannot be used, since, especially for vacancies in the O(2) sublattice, the broadening of the mainly unoccupied hybridized Bi-O(2)-O(3) states mentioned above gives rise to an increasing $n(\varepsilon_F)$. It should be noted, however, that the calculated relative changes of $n(\varepsilon_F)$ for the nonstoichiometric cases do not exceed 15% relative to the stoichiometric case.

The calculation of the O $K\alpha$ x-ray-emission and He II (40.8-eV) photoemission spectra has been performed using the same approximations as Marksteiner *et al.*[22] In the case of the O $K\alpha$ XES, however, we took into account the empirical corrections for the O 1s binding energies made by Burgäzy *et al.*[27] The calculated spectra for $Bi_2Sr_2CaCu_2O_{7.5}$ are presented in Fig. 4 as the normalized difference with respect to the ordered system. Since the He II photoemission spectrum also mainly maps O p PDOS (see Fig. 1 of Ref. 22), the two difference spectra show close similarities. Note that in order to mimic the experimental spectrometer resolution for the He II PES and the O $K\alpha$ XES a Gaussian broadening with a half-width of 0.2 and 0.55 eV, respectively, was applied. Since the decreased oxygen contribution to the intensity mainly maps the changing shape of the O p–like LDOS, the

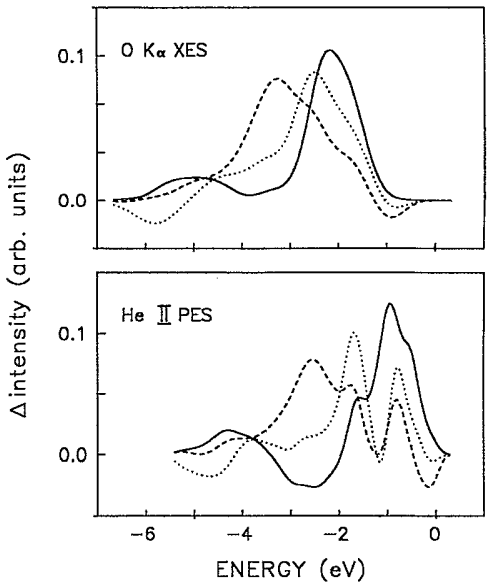

FIG. 4. Calculated O $K\alpha$ x-ray-emission and He II photoemission spectra of $Bi_2Sr_2CaCu_2O_{7.5}$ as the normalized difference with respect to $Bi_2Sr_2CaCu_2O_8$ $[\Delta I=(I_{\text{ordered}}-I_{\text{disordered}})/I^{\max}_{\text{ordered}}]$. The solid, dashed, and dotted lines denote the cases when the O(1), O(2), or O(3) sublattice is disordered.

TABLE I. Changes of the calculated Fermi energy, $\Delta\varepsilon_F$ (eV) and of the DOS at the Fermi level, $\Delta n(\varepsilon_F)$ [states/(eV cell)] in $Bi_2Sr_2CaCu_2O_{8-\delta}$ with respect to the ordered system. The column labeled CPA denotes the disordered sublattice.

CPA	δ	$\Delta\varepsilon_F$	$\Delta n(\varepsilon_F)$
O(1)	0.1	0.045	−0.206
	0.2	0.083	−0.350
	0.3	0.118	−0.445
	0.5	0.195	−0.429
O(2)	0.1	0.022	0.127
	0.2	0.045	0.258
	0.3	0.074	0.340
	0.5	0.106	0.479
O(3)	0.1	0.010	0.057
	0.2	0.036	0.050
	0.3	0.055	0.075
	0.5	0.105	0.094

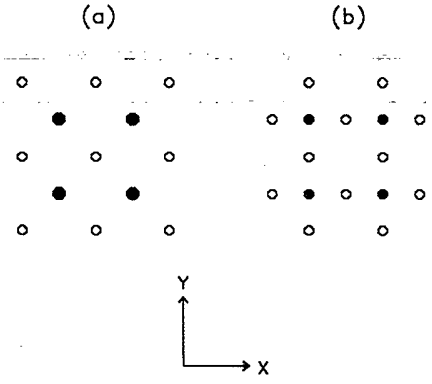

FIG. 5. Sketch of atomic positions within the (a) Bi-O or Sr-O and (b) Cu-O layers. Open circles denote oxygen sites, small solid circles denote copper sites, and large solid circles denote Bi or Sr sites.

TABLE II. Calculated effective oxygen-oxygen pair interactions, V_2^{ij} [mRy/atom] in $Bi_2Sr_2CaCu_2O_{8-\delta}$. The column headed CPA denotes the disordered sublattice. The pairs of neighbors are labeled as follows (see also, Fig. 5). O(1) sublattice: 1, first pair of neighbors; 2, second pair of neighbors with bisecting Cu site; 3, second pair of neighbors with no bisecting Cu site. O(2) or O(3) sublattice: 1, first pair of neighbors; 2, second pair of neighbors; 3, third pair of neighbors.

		V_2^{ij} pairs		
CPA	δ	1	2	3
O(1)	0.1	4.1	−3.6	−0.9
	0.3	4.2	−4.0	−0.9
	0.5	4.5	−4.1	−0.7
O(2)	0.1	−1.2	1.3	−0.8
	0.3	−3.1	−0.6	−0.4
	0.5	−4.6	−1.6	0.0
O(3)	0.1	−0.2	0.1	0.0
	0.3	−0.2	0.1	0.0
	0.5	−0.2	0.1	0.0

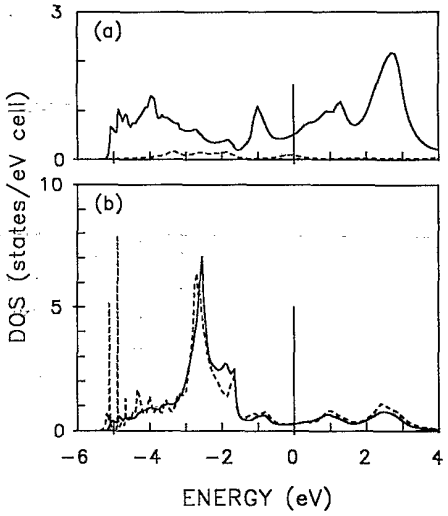

FIG. 6. (a) Bi (solid line) and Pb (dashed line) LDOS's in $Bi_{1.5}Pb_{0.5}Sr_2CaCu_2O_8$, (b) O(2) LDOS for the ordered system (dashed line) and for $Bi_{1.5}Pb_{0.5}Sr_2CaCu_2O_8$ (solid line).

difference spectra are sensitive with respect to the sublattice where vacancies are built in. In the He II photoelectron spectrum, however, an induced peak can be seen at about −0.8 eV, which is associated with a decrease of the Cu *d*-like contribution. For a deficient O(1) sublattice, this effect is amplified also by the missing O(1) contribution.

Figure 5 illustrates the arrangement of atoms in the Bi-O, Sr-O, and Cu-O layers. Due to the very minor orthorhombic distortion, the calculated effective pair interactions showed no sensitivity for corresponding pairs along the x (i.e., $\langle 100 \rangle$) and y ($\langle 010 \rangle$) directions. The results are shown in Table II. The effective O(1)-O(1) pair interactions can be correlated fairly well with the corresponding pair interactions found for the Cu-O planes of the Y-Ba-Cu-O system.[35] The pairs bisected by copper atoms again give definite negative contributions, indicating that a vacancy-(copper)-vacancy or oxygen-(copper)-oxygen type of ordering is also energetically preferred in this system. On the contrary, the positive effective interactions for the pairs with no intersecting Cu sites suggest an oxygen-vacancy (antilikewise) ordering along the $\langle 110 \rangle$ directions. For the O(2) sublattice (Bi-O layers), however, an increasing tendency of likewise ordering is found since the effective first-neighbor interactions become more and more negative with increasing vacancy content. This implies the onset of a complete phase separation on this sublattice with respect to the oxygen atoms and vacancies. Due to the very small magnitude of pair interactions, no tendency of any kind of ordering is found for the oxygen-vacancy system on the O(3) sublattice.

C. $(Bi_{1-x}Pb_x)_2Sr_2CaCu_2O_8$

Substitution of Bi with Pb has only a minor effect on the LDOS's of $Bi_2Sr_2CaCu_2O_8$. Figures 6(a) and 6(b) suggest that the Pb *p*-like states hybridized weakly with the O(2) [and O(3)] states give rise to a small Pb LDOS below ε_F. It is apparent that the sharp peaks in the Bi and O(2) LDOS's around −5 eV disappear due to the (now) disordered Bi sublattice. The breaking of the covalent Bi—O bonds leads to an increase of the O(2) states around −2 eV, while the weight of the bonding and antibonding peaks is decreased, which results in a charge localization on the O(2) sites. This is the very reason for the dropping of ε_F with increasing Pb content (Table III). Due to the Cu-O band below ε_F, $n(\varepsilon_F)$ increases considerably. The effective Bi-Bi pair energies are positive and the pairs with a bisecting O(2) sites (labeled by 2 in Table III) give

TABLE III. Changes of the calculated Fermi energy, $\Delta\varepsilon_F$ (eV) and of the DOS at the Fermi level, $\Delta n(\varepsilon_F)$ [states/(eV cell)] with respect to the ordered system as well as the effective Bi-Bi pair interactions, V_2^{ij} (mRy/atom) in $(Bi_{1-x}Pb_x)_2Sr_2CaCu_2O_8$. The first, second, and third Bi-Bi pairs of intralayer neighbors are labeled 1, 2, and 3, respectively. For visualization of the neighbors, see Fig. 5.

			V_2^{ij} pairs		
x	$\Delta\varepsilon_F$	$\Delta n(\varepsilon_F)$	1	2	3
0.05	−0.064	0.471	0.7	2.6	0.7
0.15	−0.137	1.132	0.4	3.5	0.2
0.25	−0.196	1.817	0.7	4.5	0.0

an increasing contribution as the Pb concentration increases. Thus, the Bi and Pb atoms tend to order by forming an antilikewise neighborhood in this concentration range.

IV. CONCLUSION

We have presented a systematic study of the electronic structure of $Bi_2Sr_2CaCu_2O_{8-\delta}$ and $(Bi_{1-x}Pb_x)_2Sr_2CaCu_2O_8$ in terms of the relativistic RSSC-CPA method. Pronounced differences have been found in the behavior of $n(\varepsilon_F)$ when the O(1) or the O(2) sublattices are disordered. The dropping of $n(\varepsilon_F)$ for a deficient O(1) sublattice correlates with the decreasing T_c for the nonstoichiometric system. From the effective pair interactions on this sublattice, we found indications for the creation of Cu sites with reduced oxygen coordination. The oxygen-vacancy subsystem on the O(2) sublattice shows effects of a phase separation. Based on the fairly good agreement between experiment and theory,[27] we are convinced that experimental O $K\alpha$ XES intensities can provide information about the preferential disordered sublattice.

The increasing $n(\varepsilon_F)$ in the case of Pb "doping" into the Bi sublattice may also be correlated with the experimental finding that Pb supports superconductivity in the Bi-Sr-Ca-Cu-O system associated, however, essentially with the disappearance of the structural modulations (superlattice structure) with increasing Pb content.[36] Qualitatively good confirmation of our results is provided by inverse photoemission experiments[37] and scanning tunneling spectroscopy[38] (STS) indicating a decrease of the unfilled Bi 6*p* and O 2*p* states due to the replacement of Bi by Pb.

ACKNOWLEDGMENTS

This work was supported by the Austrian Ministry of Science (Zl.49.554/1-27a/88) and the Austrian Science Foundation (P7064). The calculations were performed by using the EASI facilities of the Vienna University Computing Center.

*Present address: Institute of Physics, Technical University of Budapest, Budafoki u. 8, 1521 Budapest, Hungary.

[1]C. Michel, M. Hervieu, M. M. Borel, A. Grandin, F. Deslandes, J. Provost, and B. Raveau, Z. Phys. B **68**, 421 (1987).

[2]H. Maeda, Y. Tanaka, M. Fukutomi, and T. Asano, Jpn. J. Appl. Phys. Lett. **27**, L209 (1988).

[3]C. W. Chu, J. Bechtold, L. Gao, P. H. Hor, Z. J. Huang, R. L. Meng, Y. Y. Sun, Y. Q. Wang, and Y. Y. Xue, Phys. Rev. Lett. **60**, 941 (1988).

[4]J. M. Tarascon, Y. LePage, P. Barboux, B. G. Bagley, L. H. Greene, W. R. McKinnon, G. W. Hull, M. Giroud, and D. M. Hwang, Phys. Rev. B **37**, 9382 (1988); J. M. Tarascon, W. R. McKinnon, P. Barboux, D. M. Hwang, B. G. Bagley, L. H. Greene, G. Hull, Y. LePage, N. Stoffel, and M. Giroud, *ibid.* **38**, 8885 (1988).

[5]S. Sunshine, T. Siegrist, L. F. Schneemeyer, D. W. Murphy, R. J. Cava, R. B. vanDover, R. M. Fleming, S. H. Glarum, S. Nakahara, R. Farrow, J. J. Krajewski, S. M. Zahurak, J. V. Wasczak, J. H. Marshall, P. Marsh, L. W. Rupp, Jr., and W. F. Peck, Phys. Rev. B **38**, 893 (1988).

[6]S. M. Green, C. Jiang, Y. Mei, H. L. Luo, and C. Politis, Phys. Rev. B **38**, 5016 (1988).

[7]R. Ramesh, G. Thomas, S. M. Green, C. Jiang, Y. Mei, M. L. Rudee, and H. L. Luo, Phys. Rev. B **38**, 7070 (1988).

[8]R. Ramesh, M. S. Hedge, C. C. Chang, J. M. Tarascon, S. M. Green, and H. L. Luo, J. Appl. Phys. **66**, 4878 (1989).

[9]D. E. Morris, C. J. Hultgren, A. M. Markelz, J. Y. T. Wei, N. G. Asmar, and J. H. Nickel, Phys. Rev. B **39**, 6612 (1989).

[10]L. Forró and J. R. Cooper, Europhys. Lett. **11**, 55 (1990).

[11]G. Briceno and A. Zettl, Phys. Rev. B **40**, 11 352 (1989).

[12]M. S. Hybersten and L. F. Mattheiss, Phys. Rev. Lett. **60**, 1661 (1988).

[13]P. A. Sterne and C. S. Wang, J. Phys. C **21**, L949 (1988).

[14]F. Herman, R. V. Kasowski, and W. Y. Hsu, Phys. Rev. B **38**, 204 (1988).

[15]L. F. Mattheiss and D. R. Hamann, Phys. Rev. B **38**, 5012 (1988).

[16]H. Krakauer and W. E. Pickett, Phys. Rev. Lett. **60**, 1665 (1988).

[17]S. Massida, Jaejun Yu, and A. J. Freeman, Physica C **152**, 251 (1988).

[18]P. Steiner, S. Hüfner, A. Jungmann, S. Junk, V. Kinsinger, I. Sander, W. R. Thiele, N. Backes, and C. Politis, Physica C **156**, 213 (1988).

[19]Z.-X. Shen, P. A. P. Lindberg, I. Lindau, W. E. Spicer, C. B. Eom, and T. H. Geballe, Phys. Rev. B **38**, 7152 (1988).

[20]F. U. Hillebrecht, J. Fraxedas, L. Ley, H. J. Trodahl, J. Zaanen, W. Braun, M. Mast, H. Petersen, M. Schaible, L. C. Bourne, P. Pinsukanjana, and A. Zettl, Phys. Rev. B **39**, 236 (1989).

[21]A. J. Arko, R. S. List, R. J. Bartlett, S-W. Cheong, Z. Fisk, J. D. Thompson, C. G. Olson, A-B. Yang, R. Liu, C. Gu, B. W. Veal, J. Z. Liu, A. P. Paulikas, K. Vandervoort, H. Claus, J. C. Campuzano, J. E. Schirber, and N. D. Shinn, Phys. Scr. **T31**, 282 (1990).

[22]P. Marksteiner, S. Massidda, Jaejun Yu, A. J. Freeman, and J. Redinger, Phys. Rev. B **38**, 5098 (1988).

[23]F. Minami, T. Kimura, and S. Takekawa, Phys. Rev. B **39**, 4788 (1989).

[24]T. Takahashi, H. Matsuyama, H. Katayama-Yoshida, Y. Okabe, S. Hosoya, K. Seki, H. Fujimoto, M. Sato, and H. Inokuchi, Phys. Rev. B **39**, 6636 (1989).

[25]C. G. Olson, R. Liu, D. W. Lynch, R. S. List, A. J. Arko, B. W. Veal, Y. C. Chang, P. Z. Jiang, and A. P. Paulikas, Phys. Rev. B **42**, 381 (1990).

[26]G. Hörmandinger, P. Weinberger, P. Marksteiner, and E. Badralexe, Physica B (to be published).

[27]F. Burgäzy, C. Politis, P. Lamparter, and S. Steeb, Z. Naturforsch. A **44**, 780 (1989).

[28]L. Szunyogh, G. H. Schadler, P. Weinberger, R. Monnier, and R. Podloucky, Phys. Rev. B **41**, 1973 (1990).

[29]P. Weinberger, *Electron Scattering Theory for Ordered and Disordered Matter* (Clarendon, Oxford, 1990).

[30]A. Gonis, X.-G. Zhang, A. J. Freeman, P. Turchi, G. M. Stocks, and D. M. Nicholson, Phys. Rev. B **36**, 4630 (1987).

P. E. A. Turchi, G. M. Stocks, W. H. Butler, D. M. Nicholson, and A. Gonis, Phys. Rev. B **37**, 5982 (1988).
[31]L. Szunyogh, U. König, P. Weinberger, R. Podloucky, and P. Herzig, Phys. Rev. B **42**, 432 (1990).
[32]J. Klima, G. Schadler, P. Weinberger, and A. Neckel, J. Phys. **15**, 1307 (1985).
[33]B. Ginatempo and J. B. Staunton, J. Phys. F **18**, 1827 (1988).
[34]J. L. Beeby, Proc. R. Soc. London, Ser A **279**, 82 (1964).
[35]L. Szunyogh and P. Weinberger, Phys. Rev. B **43**, 3768 (1990).
[36]N. Fukushima, H. Niu, S. Nakamura, S. Takeno, M. Hayashi, and K. Ando, Physica C **159**, 777 (1989).
[37]W. Drube, F. J. Himpsel, G. V. Chandrashekhar, and M. W. Shafer, Phys. Rev. B **39**, 7328 (1989).
[38]X. L. Wu, Z. Zhang, Y. L. Wang, and C. M. Lieber, Science **248**, 1211 (1990).